Journal of Hazardous Materials 194 (2011) 185–192

Contents lists available at ScienceDirect

Journal of Hazardous Materials

journal homepage: www.elsevier.com/locate/jhazmat

Preparation of fluorescent nanofibrous film as a sensing material and adsorbent for Cu^{2+} in aqueous solution via copolymerization and electrospinning

Wei Wang, Qingbiao Yang*, Lei Sun, Hengguo Wang, Chaoqun Zhang, Xiaoliang Fei, Mingda Sun, Yaoxian Li*

Department of Chemistry, Jilin University, Changchun, 130021, People's Republic of China

ARTICLE INFO

Article history:
Received 20 April 2011
Received in revised form 16 July 2011
Accepted 24 July 2011
Available online 5 August 2011

Keywords:
Electrospinning
Naphthalimide
Nanofibrous film
Copper ion

ABSTRACT

Novel naphthalimide-functionalized nanofibrous film was prepared by copolymerization and electrospinning. Vinyl naphthalimide monomer was synthesized and then copolymerized with methyl methacrylate via solution polymerization. This prepared copolymer was electrospun into nanofibrous film, which is an excellent sensing material and adsorbent for Cu^{2+}. When the nanofibrous film was added into acetonitrile/aqueous solution, the presence of Cu^{2+} induces the formation of a 1:1 metal–ligand complex, which exhibits a 48 nm blue-shifted from 487 nm to 439 nm in fluorescence spectra. The fluorescent film shows high sensitivities due to the high surface area-to-volume ratio of the nanofibrous film structures. The detection limit for Cu^{2+} is 20×10^{-6} M. Furthermore, the prepared materials could be utilized as an adsorbent to remove Cu^{2+} in aqueous solution efficiently, the adsorption capacity was 10.39 mg of Cu^{2+} ions per gram of nanofibrous film. All of the results in this paper show that the naphthalimide-functionalized nanofibrous film made by electrospun technique has excellent sensitivities and adsorbent properties toward Cu^{2+} over other metal ions.

1. Introduction

Copper is a significant metal pollutant due to its widespread application and also an essential trace element in biological systems [1–4]. In aquatic environments, copper exists in particulate, colloidal and soluble states, predominantly in the forms of metal and Cu^{2+} ions [5]. Fluorescent detection of Cu^{2+} would help to clarify the cellular role of Cu^{2+} in vivo as well as to monitor the concentration of Cu^{2+} in the metal contaminated sources. So far, some progress has been achieved in the creation of a chemosensor for Cu^{2+} [6–12]. Recently, new fluorescent probes in which a metal-chelating group and fluorophore are discrete subunits of the same molecules have been successfully developed for the detection of Cu^{2+} [13–19]. However, their application in related analytical techniques in the homogeneous phase is not suitable for the separation, removal and enrichment of target species [20]. In our work, the electrospun technique was used to produce recyclable nanofibrous film for the first time. Compared with above methods, electrospun technology is more fast and effective.

Electrospinning is an effective and simple method for preparing various composite nanofibers. The electrospinning technique has been developed for the synthesis of nanofibers since 1934 [21,22]. It is a process which uses a strong electrostatic force by a high static voltage applied to a polymer solution placed into a container that has a millimetre diameter nozzle. Under applied electrical force, the polymer solution is ejected from the nozzle. After the solvents are evaporated during the course of jet spraying, the nanofibers or nanoparticles are collected on a grounded collector [23–25]. The structure and the morphology of the electrospun polymer materials, be it fibers or particles, are determined by a synergetic effect of solution parameters and electrostatic forces. Nanofibers with small diameters have a large surface area per unit mass, which can be used as a convenient package and support reagents and catalysts. Many biological colloidal particles, chemical reagents, and other particulate materials [5] can be encased inside the nanofibers of single polymers, blends, or copolymers. Electrospun polymer nanofibers provide a generally applicable material for holding and protecting particles. Nanofibrous film can have approximately 1–2 orders of magnitude more surface area than that found in continuous thin films [26,27]. It is expected that this large amount of available surface area has the potential to provide unusually high sensitivity and fast response time in sensing application [28]. And, similar fluorescence sensing investigation of this material was previously carried out on thin films [29,30]. A comparison of these techniques is expected to show that the sensitivity of the electrospun fabricated nanofibrous film would be greatly improved due to the much higher surface area-to-volume ratio than that of the known for the thin films [27].

* Corresponding authors. Tel.: +86 431 88499576; fax: +86 431 88499576.
E-mail address: yangqb@jlu.edu.cn (Q. Yang).

0304-3894/$ – see front matter © 2011 Elsevier B.V. All rights reserved.
doi:10.1016/j.jhazmat.2011.07.083

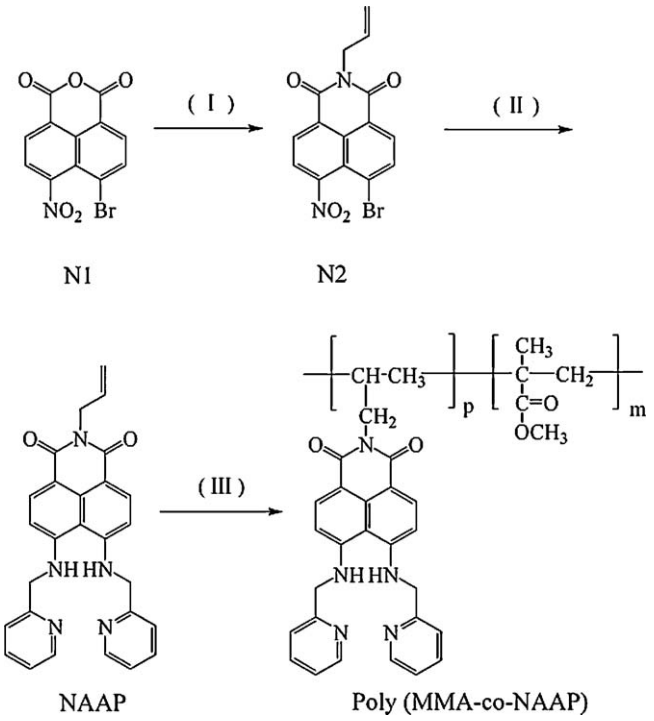

Scheme 1. Structure of NAAP and poly (MMA-co-NAAP). (I) Allyl amine, C_2H_5OH, reflux, 57.2%; (II) 2-aminomethylpyridine, $CH_3OC_2H_4OH$, CH_3CN, reflux, 46.9%; (III) MMA, DMF, AIBN, 70 °C.

1,8-Naphthalimide derivatives are one of the most efficient laser dyes and fluorescent probes because of its large molar extinction coefficient and high fluorescence quantum yield. Another approach for designing ratiometric metal ion sensors relies on the utilization of intramolecular charge transfer (ICT) processes via ICT-based fluorophores whose fluorescence emission band can shift remarkably upon binding or reacting with target metal ions [28,30–34]. ICT-induced blue shift of the emission peak will occur if the electron-donating capability of amine moieties is weakened by replacing with a less electron-rich or electron-deficient substituent [28,29,32].

In this work, novel naphthalimide-functionalized electrospun nanofibrous film was synthesized and utilized as ratiometric chemosensor and adsorbent for Cu^{2+} for the first time. The fluorescent nanofibrous film showed high sensitivity and selectivity toward Cu^{2+} over other metal ions. The sensing material poly (MMA-co-NAAP) was synthesized by copolymerizing 1,8-naphthalimide functionalized (NAAP) with methyl methacrylate (Scheme 1).

2. Experiment

2.1. Materials

Acenaphthene (97% purity, Beijing Hengyue Zongyuan Chemical Co., Ltd.) was purified by recrystallization from petroleum ether. Allyl amine (XinHua Chemical Reagent Co.) was distilled and then stored at −20 °C prior to use. *N*,*N*-Dimethylformamide (DMF) was distilled and dried by anhydrous magnesium sulfate. 2-Aminomethylpyridine (99% purity), N-bromosuccinimide (NBS), fuming HNO_3, and all other reagents were purchased from Sinopharm Chemical Reagent Co., Ltd., and used as received. The solution of metal ions were prepared from NaCl, KCl, $CaCl_2$, $MgSO_4$, $FeCl_3$, $Mn(NO_3)_2{\cdot}6H_2O$, $CoCl_2{\cdot}6H_2O$, $NiCl_2{\cdot}6H_2O$, $Zn(NO_3)_2$, $C_4H_6CdO_4{\cdot}2H_2O$, $CuCl_2{\cdot}2H_2O$, $Hg(NO_3)_2$, $AgNO_3$, $Pb(NO_3)_2$, respectively, and were dissolved in deionized water.

2.2. Characterization

^1H NMR spectra were measured on a Bruker AV-400 spectrometer with chemical shifts reported as parts per million (in $CDCl_3$, TMS as internal standard). IR spectra were recorded on a Bruker Vector-22 spectrometer. The pH values of the test solution were measured with a glass electrode connected to a Mettler-Toledo Instruments DELTA 320 pH meter (Shanghai, China) and adjusted if necessary. Fluorescence spectra were determined on a Hitachi F-4500. UV–Vis spectra were recorded on a Hitachi U-3010 UV-Vis spectrophotometer. High voltage power (0–50 kV) DW-P503-1AC (Tianjin, China). Scanning electron microscope (SEM), SII: SPI3800N (Japan).

2.3. Synthesis of N-allyl -4-bromo-5-nitro-1, 8-naphthalimide (N2)

4-Bromo-5-nitro-1,8-naphthalic anhydride (N1) was synthesized from acenaphthene via a literature procedure [30]. Allyl amine (57 mg, 1.00 mmol) in ethanol (10 mL) was added dropwise, under mechanical stirring, to solution of 4-bromo-5-nitro-1,8-naphthalic anhydride (N1) (300 mg, 0.93 mmol) in ethanol (40 mL). The reaction mixture was refluxed for 4 h and then cooled. After the removal of the solvent, the crude product was purified by column chromatography (silica gel, CH_2Cl_2/EtOH, 20:1) to give compound N2 as a white solid (192 mg, 57.2%).

2.4. Synthesis of N-allyl-4, 5-di [(2-picolyl) amino]-1, 8naphthalimide (NAAP)

By adopting a literature procedure for similar compounds [32], 2-(aminomethyl)pyridine (300 mg, 2.77 mmol) was added dropwise under stirring to a solution of N-(4-hydroxyphenethyl)-4-bromo-5-nitro-1,8-naphthalimide (100 mg, 0.28 mmol) in 2-methoxyethanol (10.0 mL). Then the mixture was heated to reflux for 5 h under a nitrogen atmosphere. After cooling to room temperature, the chloroform solution was removed by vacuum roto-evaporation and purified by column chromatography (silica gel, CH_2Cl_2/MeOH, 10:1, v/v) to give a yellow solid (59 mg, 46.9%). 1H NMR ($CDCl_3$, 300 MHz) δ 3.47 (t, 1H), 3.70–3.75 (t, 2H), 4.65 (m, 2H), 5.12–5.28 (m, 2H), 5.92–6.05 (m, 1H), 6.78 (d, 2H), 7.15–7.40 (m, 2H), 7.62–7.72 (m, 2H), 8.28 (d, 2H), 8.42 (d, 2H). IR (KBr, cm^{-1}): 3552, 3438, 2995, 2356, 2336, 1728, 1640, 1486, 1441, 1384, 1270, 1149, 1096, 986, 963, and 751. HRMS (ESI) calcd for $C_{27}H_{23}N_5O_2$. [MH^+]: 450.0.

2.5. Synthesis of poly (MMA-co-NAAP)

Poly (MMA-co-NAAP) was prepared by the copolymerization of NAAP and MMA with AIBN as a thermal initiator. Briefly, 0.18 g (4.0×10^{-4} mol) NAAP, 2.0 g (2.0×10^{-2} mol) of MMA, and 0.03 g (2.0×10^{-2} mol) of AIBN in 10 mL of DMF were introduced into a dry polymerization tube. The solution was deoxygenated by purging with N_2 gas for 5 min. The tube was sealed and placed in a regulated thermostat bath at 70 °C for 24 h. The obtained poly (MMA-co-NAAP) was transparent and colored. It was dissolved in $CHCl_3$ (20 mL) and precipitated with CH_3OH (200 mL). After successive dissolving and precipitation (4 times), the colored PMMA was filtrated on a glass filter and dried under vacuum at 50 °C to a constant weight. The molar concentration of the dye molecules in the copolymer was 0.89% as determined by ultraviolet spectrophotometry.

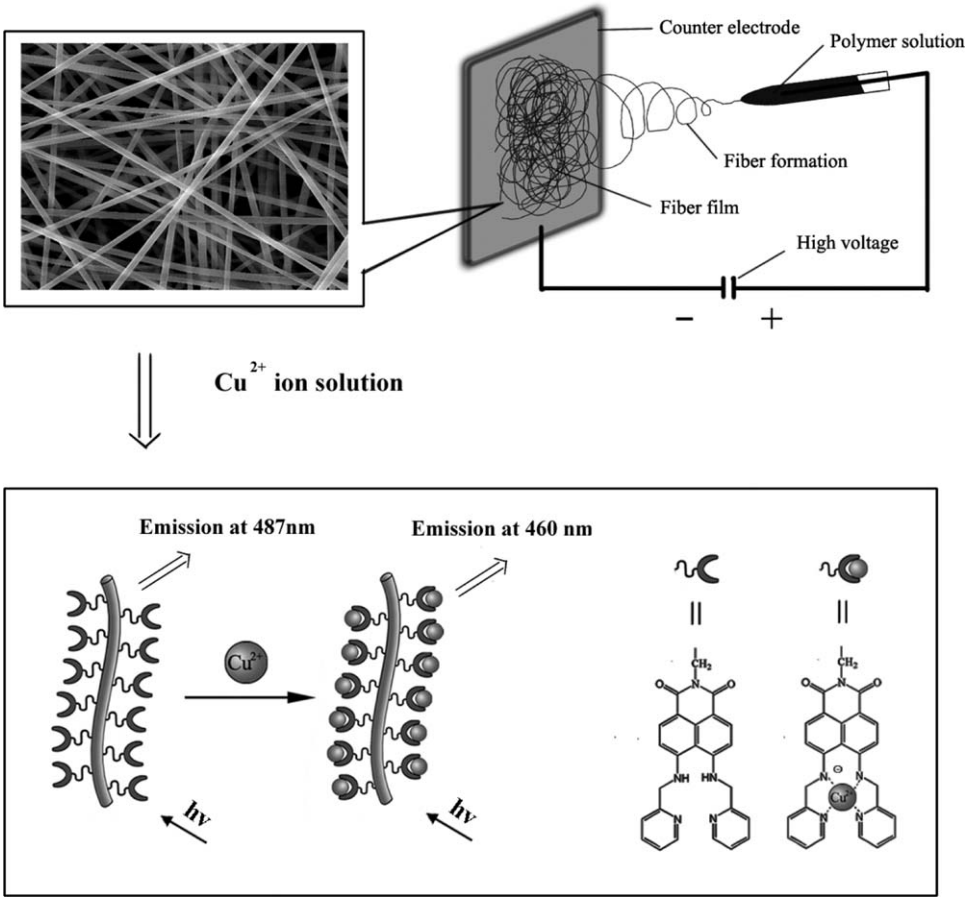

Scheme 2. Schematic illustration for preparation of poly (MMA-co-NAAP) nanofiber fluorescent sensors by electrospinning for Cu^{2+} ions with enhanced detection sensitivity.

2.6. Preparation of electrospinning solution and film

Poly (MMA-co-NAAP) of 0.8 g was added to 2.4 g DMF solution to prepare precursor solution with a concentration of 25 wt%. The solution was rapidly stirred for 24 h at room temperature. The resulting clear homogenous solution was used for electrospinning the film.

A burette with an inserted Cu rod to connect the high-voltage supply was filled with the precursor solution. An aluminum foil served as the counter electrode. The distance between the burette tip and receiver was fixed at 17 cm. The high-voltage supply was fixed at 15 kV. The spinning rate was controlled at about 4 mL/h by adjusting the angle of inclination of the burette. The electrospinning was performed at 25 °C. Scheme 2 shows the electrospinning apparatus used.

3. Results and discussion

3.1. Synthesis of poly (MMA-co-NAAP) nanofibers

Synthetic routes employed for the preparation of novel vinyl 1,8-naphthalimide-based Cu^{2+} ion sensitive fluorescent monomer (NAAP) and fluorescent nanofibrous film via copolymerization and electrospinning are shown in Schemes 1 and 2. The reaction of acenaphthene with N-bromosuccinimide and fuming nitric acid leads to 4-bromo-5-nitro-1,8-naphthalic anhydride (N1) with a yield of 87%. The compound N2 was obtained by the reaction of compound N1 with allyl amine. In the final step, the target vinyl naphthalimide monomer (NAAP) was obtained by the reaction of compound N2 with 2-(aminomethyl) pyridine. The chemical structure of NAAP was confirmed by ^{1}H NMR analysis. Poly (MMA-co-NAAP) was prepared by the copolymerization of NAAP and MMA with AIBN as a thermal initiator. Poly (MMA-co-NAAP) nanofibers prepared via electrospinning. The chemical structures and morphologies of poly (MMA-co-NAAP) nanofibers were confirmed by FT-IR analysis and SEM.

3.2. FT-IR investigations of poly (MMA-co-NAAP) film

The FT-IR spectra of poly (MMA-co-NAAP), pure PMMA and monomer NAAP are shown in Fig. 1. The spectrum of poly (MMA-co-NAAP) differs considerably from that of pure PMMA in a range of 1600–1700 cm^{-1}.The bands at 1696 cm^{-1} and 1670 cm^{-1} are assigned to the stretching vibration of C=O in amide compounds. The bands at 1270 cm^{-1} and 1096 cm^{-1} are assigned to the stretching vibrations of the C–O–C bond. Compared with that of monomer NAAP, the absorption band at 1640 cm^{-1} the characteristic for the C=C vibrations from the allyl group disappeared. From the FT-IR spectra of the poly(MMA-co-NAAP) nanofibers, the introduction of NAAP into PAN nanofibers was confirmed.

3.3. Morphologies of poly (MMA-co-NAAP) nanofibers

A typical SEM image of a poly (MMA-co-NAAP) nanofibrous film is shown in Fig. 2. It can be seen that the film was composed of numerous, randomly oriented nanofibers. In this work, the beads on the fibers were formed during electrospinning of a 15 wt% poly (MMA-co-NAAP) solution. The beads disappeared as concentration increased from 22 to 25 wt%. The surface of the poly (MMA-co-NAAP) (25 wt%) nanofibrous film did not show any serious cracks

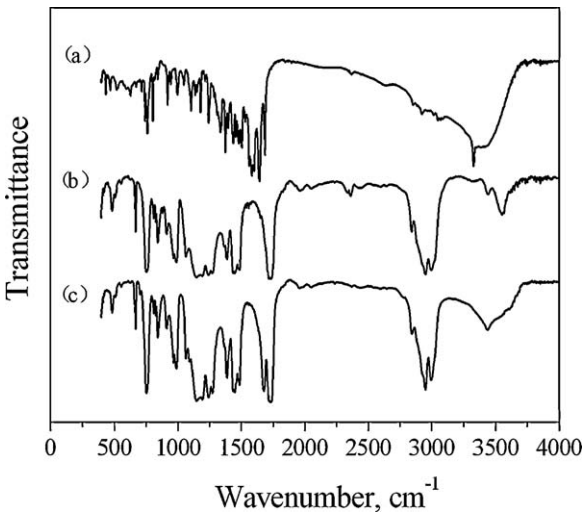

Fig. 1. FT-IR spectra of (a) NAAP, (b) pure PMMA, and (c) poly (MMA-co-NAAP).

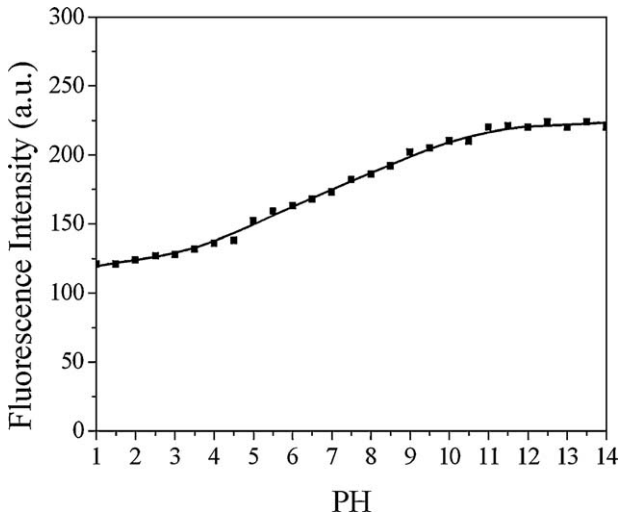

Fig. 3. Fluorescence emission of nanofibrous film (1.4 cm × 3.5 cm) in an acetonitrile–water (1:1, v/v) solution at different pH values, excitation wavelength was 400 nm. pH was adjusted by 75% $HClO_4$ and NaOH.

or degradation and presented an almost similar morphology to that of pure PMMA nanofibers (Fig. 2(a)). The diameter of the nanofibers increased with an increase in the concentration of poly (MMA-co-NAAP) solution due to an increase in viscosity, and ranged between 250 and 350 nm as shown in Fig. 2(b). In this work, the average diameter (D) of nanofibers can be estimated in the following equation:

$$D = \frac{1}{n}\sum_{i=1}^{n} X_i^* \frac{B}{L} \quad (1)$$

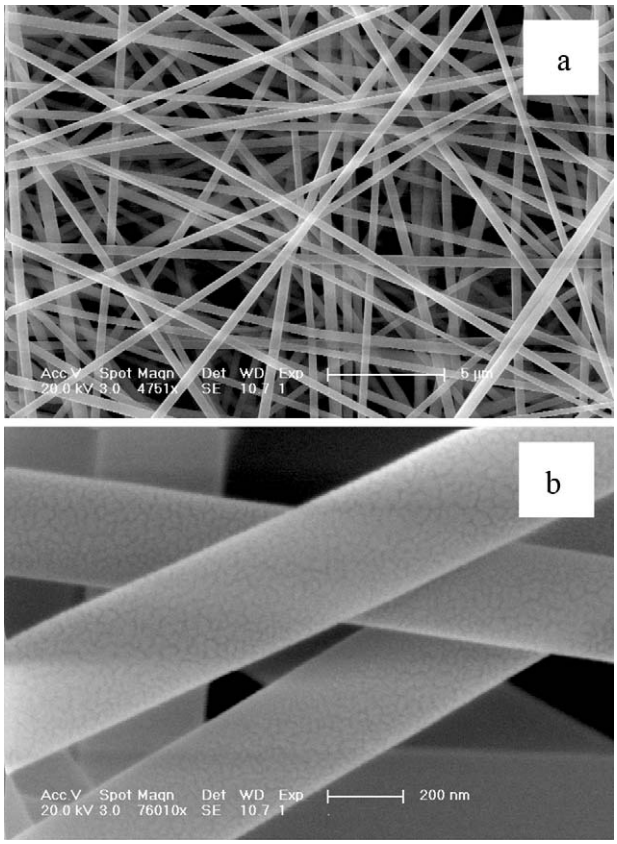

Fig. 2. SEM images of poly (MMA-co-NAAP) nanofiber (a) and further magnified image of several poly (MMA-co-NAAP) electrospun nanofibers (b).

where n stands for the number of the nanofibers in SEM images, X stands for the diameter of each nanofiber, B is the scale bar, and L refers to the length of the scale bar. Therefore, the average diameter of poly (MMA-co-NAAP) nanofibers was 311 nm. This type of network structure of the electrospun film provides a surface area-to-volume ratio roughly 1–2 orders of magnitude higher than that of known continuous thin films [27]. Further higher surface area-to-volume ratio may be achieved by changing the conditions of the electrospinning process such as solvent, concentration, and working distance, which result in either smaller diameter fibers or increased porosity on the fiber surface [30].

3.4. The effect of pH

Fluorophores are usually disturbed by the protons in the detection of metal ions, so their low sensitivity to the operational pH value was expected and investigated. The fluorescence emission intensities of poly (MMA-co-NAAP) nanofibrous film in acetonitrile–water (1:1, v/v) as a function of pH are shown in Fig. 3. It was found that, the pH has some effect on the fluorescence emission intensity of the poly (MMA-co-NAAP) nanofibrous film. And the fluorescence emission intensity increases with the increment of the pH, which can be ascribed that the hydrogen bond interaction between the amino proton and hydroxide enhances the intramolecular charge transfer (ICT) of receptor poly (MMA-co-NAAP) nanofibrous film. This is the same as that described by literature [32]. Considering that most samples for Cu^{2+} ions analysis were neutral, therefore, the media for Cu^{2+} ions quantification was then buffered at pH 7.2.

3.5. Response of poly (MMA-co-NAAP) nanofibrous film to Cu^{2+} ions

In order to gain an insight into the signaling properties of the film toward Cu^{2+}, fluorescence titrations were conducted. The fluorescence titration behavior of the film was investigated in an acetonitrile–water (1:1, v/v) solution ([Cu^{2+}] = 0–20 μM, 0.1 M KH_2PO_4–NaOH buffer at pH 7.20). When Cu^{2+} was added to the solution of the film, a significant decrease in the emission wavelength at 487 nm and a blue shift in the emission maximum from 487 to 439 nm were observed (Fig. 4). When more Cu^{2+} was added, the maximum fluorescence intensity was not increased further. Significantly, the intensity at 439 nm increased with the

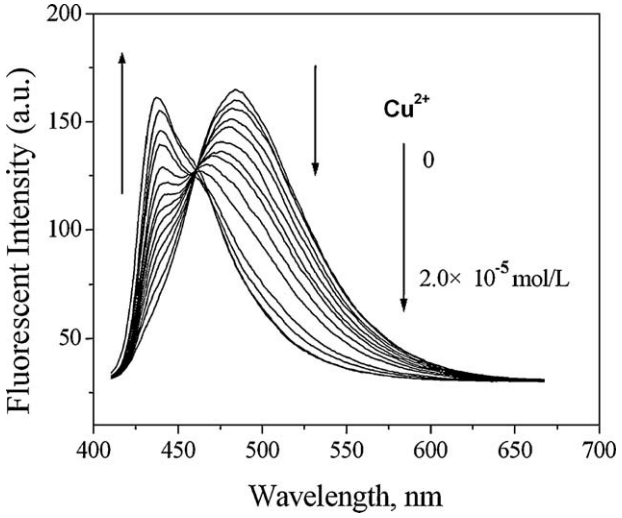

Fig. 4. Fluorescent emission spectra of the film in the presence of Cu^{2+} (0–20 μM) at different concentrations of in acetonitrile–water solution (1:1, v/v, 0.1 M KH_2PO_4–NaOH buffer at pH 7.20). Excitation wavelength was 400 nm, and emission was at 439 and 487 nm.

increased concentration of Cu^{2+} up to a mole ratio (NAAP/Cu^{2+}) of 1:1 (Scheme 2) [32,35]. The change in solution for blue-shifted fluorescence spectra from 487 nm to 439 nm was attributed to the deprotonation of the secondary amine conjugated to the naphthalene ring [32,34]. The nanofibrous film sensing material for Cu^{2+} was developed from recent sensor for Cu^{2+} on the base of the same deprotonation mechanism [36,37]. We plotted the changes in fluorescence emission intensity at 439 nm (solid) and 487 nm (open) as a function of Cu^{2+} concentration (Fig. 5a). When more than 20 μm Cu^{2+} was added, the maximum fluorescence intensity was retained. Significantly, the intensity at 532 nm increased linearly with the concentration of Cu^{2+} (linearly dependent coefficient: $R^2 = 0.9908$) (Fig. 5b), which indicated that nanofibrous film had potential use for the quantitative determination of Cu^{2+}.

The nanofibrous film exhibited the high sensitivity to Cu^{2+} ion in the 2.0×10^{-5}–1.0×10^{-3} M response range. Too little copper ion, shown for 1 μM copper ion, and the nanofibrous film will not respond to the full range. Too much copper ion, shown for 10 mM copper ion, and the total fluorescent response range is reduced. The static response time of the nanofibrous film was <30 s ([Cu^{2+}] = 0–20 μM), the higher concentration required a longer response time. In terms of lifetime of the poly (MMA-co-NAAP) nanofibrous film, their response stability was observed for over more than three months.

In addition, when ETDA was added to the sensing system, the fluorescent spectra were recovered. The result indicated that the Cu^{2+}-induced deprotonation reaction was reversible. Over three times reuse, the fluorescence intensity values of nanofibrous film (at 487 nm) were respectively 156 (97.5%), 149 (92%), 141 (87%). Recovery test showed that the nanofibrous film could be reproduced for three times without losing its sensitivity. After three times, may be due to the film damage resulting fluorescence decreased. The results indicated that the regeneration ability of the nanofibrous film was satisfactory.

3.6. Response of poly (MMA-co-NAAP) nanofibrous film to various metal ions

The fluoroionophoric behavior of poly (MMA-co-NAAP) nanofibrous film was investigated in an acetonitrile–water (1:1, v/v) solution ([M^+] = 20 μM, 0.1 M KH_2PO_4–NaOH buffer at pH 7.20). The fluorescence titration of the film with various metal ions was conducted to examine the selectivity of the film. As expected, the film showed a weak fluorescence in an acetonitrile–water solution. Upon addition of different metal ions, only Cu^{2+} can induce remarkable fluorescence blue-shift of the nanofibrous film (Fig. 6). Fig. 7(a) shows that the dependence of the intensity ratios is given as a function of the logarithm of Cu^{2+} ion concentration. The fluorescence emission intensity at 439 nm increased about homology with film equivalent of Cu^{2+} ion. Other representative metal ions, such as Hg^{2+}, Zn^{2+}, Na^+, Li^+, Pb^{2+}, Zn^{2+}, Cd^{2+}, Fe^{2+}, Pb^{2+}, Ag^+, Mn^{2+}, Co^{2+}, Ni^{2+} ions, showed almost negligible effects on the fluorescence behavior of the film. The competition experiments were conducted in the presence of Cu^{2+} ion mixed with Pb^{2+}, Mg^{2+}, Na^+, K^+, Li^+, $Cd2^+$, Ca^{2+}, Fe^{2+}, Co^{2+}, Ni^{2+}, Zn^{2+}, Hg^{2+}, Ag^+ and Mn^{2+}, as well as in a mixture of the metal ions, respectively; no significant spectral change in the intensity ratios ($I439/I487$) was found by comparison with that without the other metal ions besides Cu^{2+} (Fig. 7(b)). The competition experiments revealed that nanofibrous film showed a remarkable selectivity toward Cu^{2+} over other competitive cations.

3.7. Adsorption kinetics of Cu^{2+} ions onto poly (MMA-co-NAAP) nanofibrous film

Almost all current Cu^{2+} sensors can only detect the heavy metal ions, but not remove them from solution. In this work, we endowed

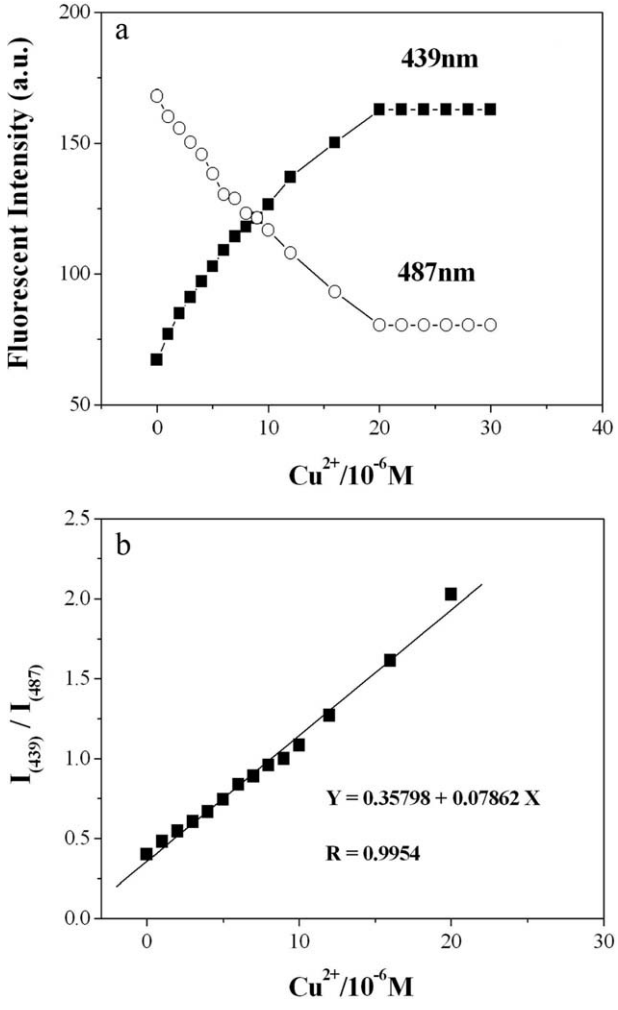

Fig. 5. (a) Fluorescent emission response of the film at 439 nm (solid) and 487 nm (open) as a function of Cu^{2+} concentration and (b) the linear dependence of the film within the concentration of Cu^{2+} (0–20 μM).

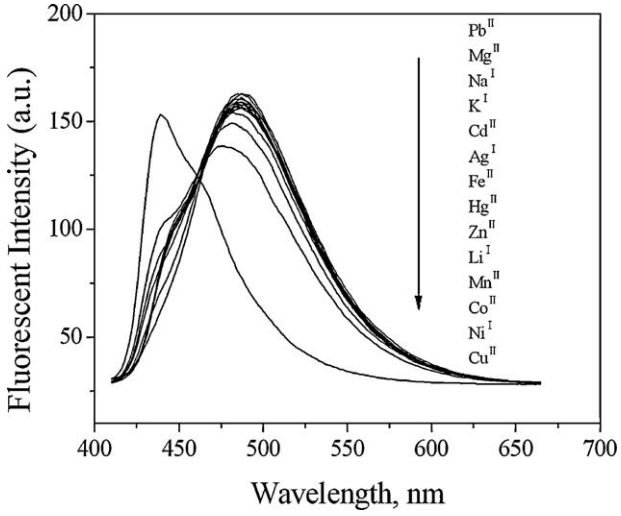

Fig. 6. Fluorescence spectra of the film to different metal ions in acetonitrile–water solutions (1:1, v/v, 20 μM, pH = 7.20).

the nanofibrous film with adsorptive and separable properties to remove the Cu^{2+} ions from aqueous solution.

The metal-loaded poly (MMA-co-NAAP) nanofibrous film (size: 1.4 cm × 3.5 cm, weight: 0.0215 ± 0.0005 g) was added to an HNO_3 solution of 1 mol/L. 1 mol/L HNO_3 was added to an aqueous solution containing different concentrations of Cu^{2+} ions [38,39]. Fig. 8(a)

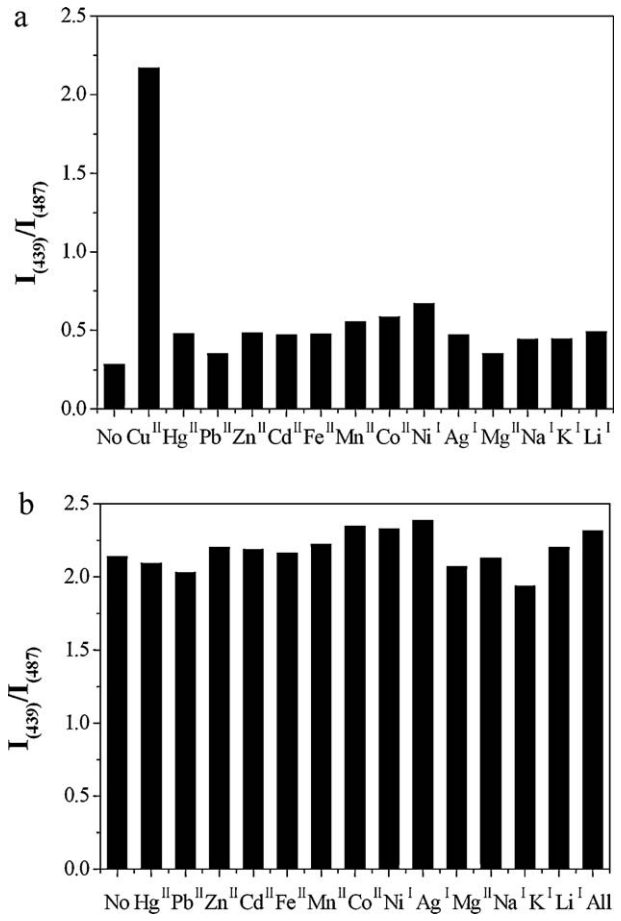

Fig. 7. (a) Fluorescent emission response of the film in the presence of different metal ions in an acetonitrile–water solution (1:1, v/v, 20 μM, pH = 7.20) and (b) fluorescent response of the film to the selected metal ions (20 μM).

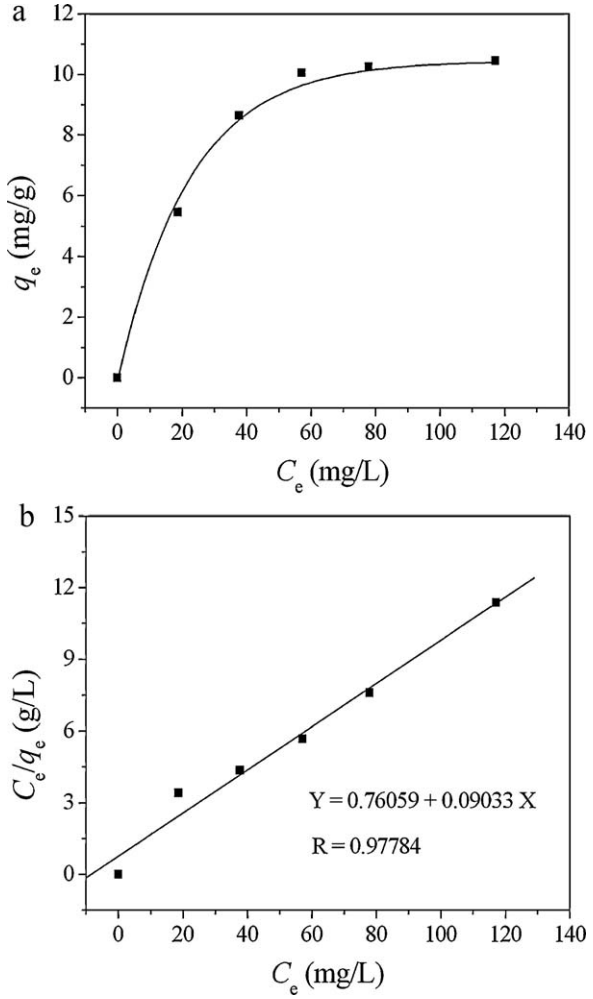

Fig. 8. (a) Adsorption isotherm and (b) Langmuir plot of Cu^{2+} on the poly (MMA-co-NAAP) nanofibrous film.

illustrates the equilibrium adsorption amounts at 24 h under various equilibrium concentrations. It was found that the adsorption of Cu^{2+} increased initially with the increase in concentration and then leveled off. The initial increase in metal adsorption might be due to many available chelating sites on the poly (MMA-co-NAAP) nanofibrous film [40]. The concentration of Cu^{2+} ions left in aqueous solution was determined by inductively coupled plasma mass spectrometry (ICP-MS). The experimental adsorption equilibrium data of Cu^{2+} was analyzed according to the Langmuir adsorption equation, which is given as follows [41].

$$\frac{C_e}{q_e} = \frac{1}{K_L q_m} + \frac{C_e}{q_m} \quad (2)$$

where q_e is the equilibrium quantity of the metals ions adsorbed onto the poly (MMA-co-NAAP) nanofibrous film (mg/g), C_e is the equilibrium concentration (mg/L), and q_m (mg/g), and K_L (L mg^{-1}) are the Langmuir constants related to the saturation adsorption capacity and binding energy (affinity), respectively. Fig. 8(b) shows the Langmuir C_e/q_e versus C_e plot with good linear relationship (R^2 over 0.95) found. The basic assumption of the Langmuir theory is that adsorption takes place at specific homogeneous sites within the adsorbent and once a metal ion occupies a reaction site, then no further adsorption occurs at that location. Thus, monolayer adsorption happened on the poly (MMA-co-NAAP) nanofibrous film [41–44]. The values of q_m and K_L in Table 1 were calculated from the slope and intercept of the C_e/q_e versus C_e plot in Fig. 8(b).

Table 1
The Langmuir constants for Cu^{2+} on poly (MMA-co-NAAP) nanofibrous film.

Metal ion	K_L/L mg^{-1}	q_m/mg/g	R^2
Cu^{2+}	63.0902	10.3978	0.9562

The linear plot indicates that Cu^{2+} ion adsorption followed the Langmuir isotherm. The basic assumption of the Langmuir theory is that adsorption takes place at specific homogeneous sites within the adsorbent [45]. The adsorption capacity was 10.39 mg of Cu^{2+} ions per gram of adsorbent film (Table 1).

4. Conclusions

We have successfully developed a fluorescent nanofibrous film as a sensing material and adsorbent for Cu^{2+} in aqueous solution via copolymerization and electrospinning. The results revealed that the nanofibrous film possessed a high selectivity and sensitivity for Cu^{2+}, achieving a detection limit at the nanomolar level. In aqueous solution, the adsorption capacity was more than 10 mg of Cu^{2+} ions per gram of nanofibrous film. In summary, this nanofibrous film makes it possible to detect and remove the Cu^{2+} metrically with solid material from waste water. Further efforts will focus on exploring new sensing materials and optimizing the capability to the adsorption of analyte.

Acknowledgements

The authors gratefully acknowledge the support of the National Natural Science Foundation of China (No. 20874033), Research Fund for the Doctoral Program of Higher Education of China (No. 20100061110008).

References

[1] S. Kumar, P. Singh, S. Kaur, A Cu^{2+} protein cavity mimicking fluorescent chemosensor for selective Cu^{2+} recognition: tuning of fluorescence quenching to enhancement through spatial placement of anthracene unit, Tetrahedron 63 (2007) 11724–11732.
[2] N. Kaur, S. Kumar, Colorimetric recognition of Cu(II) by (2-dimethylaminoethyl)amino appended anthracene-9,10-diones in aqueous solutions: deprotonation of aryl amine NH responsible for colour changes, Dalton Trans. (2006) 3766–3771.
[3] Q. Donga, J. Liu, L. Songa, G. Shao, Novel zwitterionic inorganic–organic hybrids: synthesis of hybrid adsorbents and their applications for Cu^{2+} removal, J. Hazard. Mater. 186 (2011) 1335–1342.
[4] Q. Chang, M. Zhanga, J. Wanga, Removal of Cu^{2+} and turbidity from wastewater by mercaptoacetyl chitosan, J. Hazard. Mater. 169 (2009) 621–625.
[5] L.M. Hansen, D.J. Smith, D.H. Reneker, W. Kataphinan, Water absorption and mechanical properties of electrospun structured hydrogels, J. Appl. Polym. Sci. 95 (2005) 427–434.
[6] G.J. Mohr, I. Klimant, U.E. Keller, O.S. Wolfbeis, Fluoro reactands and dual luminophore referencing: a technique to optically measure amines, Anal. Chem. 73 (2001) 1053–1056.
[7] R. Sheng, P. Wang, Y. Gao, Y. Wu, W. Liu, J. Ma, H. Li, S. Wu, Colorimetric test kit for Cu^{2+} detection, Org. Lett. 10 (2008) 5015–5018.
[8] S. Goswami, D. Sen, N.K. Das, G. Hazra, Highly selective colorimetric fluorescence sensor for Cu^{2+}: cation-induced 'switching on' of fluorescence due to excited state internal charge transfer in the red/near-infrared region of emission spectra, Tetrahedron Lett. 51 (2010) 5563–5566.
[9] H.Y. Lee, D.R. Bae, J.C. Park, H. Song, W.S. Han, J.H. Jung, A selective fluoroionophore based on BODIPY-functionalized magnetic silica nanoparticles: removal of Pb2+ from human blood, Angew. Chem. Int. Ed. 48 (2009) 1239–1243.
[10] R. Corradini, A. Dossena, G. Galaverna, R. Marchelli, A. Panagia, G. Sartor, Fluorescent chemosensor for organic guests and copper(II) ion based on dansyldiethylenetriamine-modified β-cyclodextrin, J. Org. Chem. 62 (1997) 6283–6289.
[11] R. Krämer, Fluorescent chemosensors for Cu^{2+} ions: fast, selective, and highly sensitive, Angew. Chem. Int. Ed. 37 (1998) 772–773.
[12] A. Torrado, G.K. Walkup, B. Imperiali, Exploiting polypeptide motifs for the design of selective Cu(II) ion chemosensors, J. Am. Chem. Soc. 120 (1998) 609–610.
[13] J.M. Liu, Q.Y. Zheng, J.L. Yang, C.F. Chen, Z.F. Huang, A new fluorescent chemosensor for Fe^{3+} and Cu^{2+} based on calix [4] arene, Tetrahedron Lett. 43 (2002) 9209–9212.
[14] T. Gunnlaugsson, J.P. Leonard, N.S. Murray, Highly selective colorimetric naked-eye Cu(II) detection using an azobenzene chemosensor, Org. Lett. 6 (10) (2004) 1557–1560.
[15] H. Yang, Z.Q. Liu, Z.G. Zhou, E.X. Shi, F.Y. Li, Y.K. Du, T. Yi, C.H. Huang, Highly selective ratiometric fluorescent sensor for Cu(II) with two urea groups, Tetrahedron Lett. 47 (2006) 2911–2914.
[16] L. Fabbrizzi, M. Licchelli, A. Poggi, D. Sacchi, C. Zampa, A chromogenic penta-aza scorpionand for nickel (II) and copper (II) ions, Polyhedron 23 (2004) 373.
[17] S.H. Lee, J. Kumar, S.K. Tripathy, Thin film optical sensors employing polyelectrolyte assembly, Langmuir 16 (26) (2000) 10482–10489.
[18] N.E. Agbor, M.C. Petty, A.P. Monkman, Polyaniline thin films for gas sensing, Sens. Actuators B 28 (1995) 173–179.
[19] B. Liu, H. Tian, A selective fluorescent ratiometric chemo-dosimeter for mercury ion, Chem. Commun. 315 (2005) 6–3158.
[20] F. Lupo, S. Gentile, F.P. Ballistreri, G.A. Tomaselli, M.E. Fragal, A. Gulino, Viable route for switching of an engineered silica surface using Cu^{2+} ions at sub-ppm levels, Analyst 135 (2010) 2273–2279.
[21] A. Formhals, Process and apparatus fob pbepabing. US Patent No. 1975504 (1934), pp. 1–4.
[22] L. Sun, X. Yu, M. Sun, H. Wang, S. Xu, J.D. Dixon, Y.A. Wang, Y. Li, Q. Yang, X. Xu, Preparation of quantum dots encoded microspheres by electrospray for the detection of biomolecules, J. Colloid Interface Sci. 358 (2011) 73–80.
[23] D.H. Reneker, I. Chun, Nanometre diameter fibres of polymer, produced by electrospinning, Nanotechnology 7 (1996) 216–223.
[24] H.X. He, C.Z. Li, N.J. Tao, Conductance of polymer nanowires fabricated by a combined electrodeposition and mechanical break junction method, Appl. Phys. Lett. 78 (2001) 811–813.
[25] R. Sen, B. Zhao, D. Perea, M.E. Itkis, H. Hu, J. Love, E. Bekyarova, R.C. Haddon, Preparation of single-walled carbon nanotube reinforced polystyrene and polyurethane nanofibers and membranes by electrospinning, Nano Lett. 4 (2004) 459–464.
[26] X.J. Peng, J.J. Du, J.L. Fan, J.Y. Wang, Y.K. Wu, J.Z. Zhao, S.G. Sun, T. Xu, A Selective fluorescent sensor for imaging Cd^{2+} in living cells, J. Am. Chem. Soc. 129 (2007) 1500–1501.
[27] X. Wang, C. Drew, S.H. Lee, K.J. Senecal, J. Kumar, L.A. Samuelson, Electrospun nanofibrous membranes for highly sensitive optical sensors, Nano Lett. 2 (11) (2002) 1273–1275.
[28] D. Srikun, E.W. Miller, D.W. Dornaille, C.J. Chang, An ICT-based approach to ratiometric fluorescence imaging of hydrogen peroxide produced in living cells, J. Am. Chem. Soc. 130 (2008) 4596–4597.
[29] C. Li, S. Liu, Responsive nanogel-based dual fluorescent sensors for temperature and Hg^{2+} ions with enhanced detection sensitivity, J. Mater. Chem. 20 (2010) 10716–10723.
[30] J.M. Deitzel, J. Kleinmeyer, D. Harris, N.C. Tan, The effect of processing variables on the morphology of electrospun nanofibers and textiles, Polymer 42 (2001) 261–272.
[31] B. Leng, L. Zou, J.B. Jiang, H. Tian, Colorimetric detection of mercuric ion (Hg^{2+}) in aqueous media using chemodosimeter-functionalized gold nanoparticles, Sens. Actuators B 140 (2009) 162–169.
[32] Z. Xu, Y. Xiao, X. Qian, J. Cui, D. Cui, Ratiometric and selective fluorescent sensor for Cu^{II} based on internal charge transfer (ICT), Org. Lett. 7 (2005) 889–892.
[33] Y. Shiraishi, S. Sumiya, T. Hirai, A coumarin-thiourea conjugate as a fluorescent probe for Hg(II) in aqueous media with a broad pH range 2–12, Org. Biomol. Chem. 8 (2010) 1310–1314.
[34] Z. Xu, X. Qian, J. Cui, R. Zhang, Exploiting the deprotonation mechanism for the design of ratiometric and colorimetric Zn^{2+} fluorescent chemosensor with a large red-shift in emission, Tetrahedron 62 (2006) 10117–10122.
[35] H. Takakusa, K. Kikuchi, Y. Urano, K. Sakamoto, T. Yamaguchi, Nagano, Design and synthesis of an enzyme-cleavable sensor molecule for phosphodiesterase activity based on fluorescence resonance energy transfer, J. Am. Chem. Soc. 124 (2002) 1653–1657.
[36] K. Rurack, S. Acta, Flipping the light switch 'ON'-the design of sensor molecules that show cation-induced fluorescence enhancement with heavy and transition metal ions, Spectrochim. Acta Part A 7 (2001) 2161–2195.
[37] Z. Xu, X. Qian, J. Cui, Colorimetric and ratiometric fluorescent chemosensor with a large red-shift in emission: Cu(II)-only sensing by deprotonation of secondary amines as receptor conjugated to naphthalimide fluorophore, Org. Lett. 7 (2005) 3029–3032.
[38] S. Haider, S.Y. Park, Preparation of the electrospun chitosan nanofibers and their applications to the adsorption of Cu(II) and Pb(II) ions from an aqueous solution, J. Membr. Sci. 328 (2009) 90–96.
[39] C. Ramazan, S. Cengiz, S. Mehmet, Adsorption of copper(II), nickel(II) and cobalt(II) ions from aqueous solution by methacrylic acid/acrylamide monomer mixture grafted poly(ethylene terephthalate) fiber, Sep. Purif. Technol. 49 (2006) 107–114.
[40] K. Saeed, S. Haider, T.J. Oh, S.Y. Park, Preparation of amidoxime-modified polyacrylonitrile (PAN-oxime) nanofibers and their applications to metal ions adsorption, J. Membr. Sci. 322 (2008) 400–405.
[41] S. Deng, R. Bai, J.P. Chen, Behaviors and mechanisms of copper adsorption on hydrolyzed polyacrylonitrile fibers, Colloid Interface Sci. 260 (2003) 265–272.

[42] E. Pehlivan, T. Altuna, S. Parlayıcıa, Utilization of barley straws as biosorbents for Cu^{2+} and Pb^{2+} ions, J. Hazard. Mater. 164 (2009) 982–986.
[43] Z.Y. Hea, H.L. Niea, C.B. Whiteb, L.M. Zhua, Y.T. Zhoua, Y. Zhenga, Removal of Cu^{2+} from aqueous solution by adsorption onto a novel activated nylon-based membrane, J. Hazard. Mater. 99 (2008) 7954–7958.
[44] T.C. Hsu, Experimental assessment of adsorption of Cu^{2+} and Ni^{2+} from aqueous solution by oyster shell powder, J. Hazard. Mater. 171 (2009) 995–1000.
[45] I.D. Mall, V.C. Srivatava, N.K. Agarwal, Removal of orange-G and methyl violet dyes by adsorption onto bagasse fly ash-kinetic study and equilibrium isotherm analyses, Dyes Pigments 69 (2006) 210–223.